Numerical Method for 3D Quantification of Glenoid Bone Loss*

Alexander Malyshev[1] and Algirdas Noreika[2]

[1] Department of Mathematics, University of Bergen, PB 7803, 5020 Bergen, Norway
Corresponding author: alexander.malyshev@uib.no
[2] Indeform, K. Petrausko st. 26, LT-44156, Kaunas, Lithuania
algirdas.noreika@indeform.com

Abstract. Let a three-dimensional ball intersect a three-dimensional polyhedron given by its triangulated boundary with outward unit normals. We propose a numerical method for approximate computation of the intersection volume by using voxelization of the interior of the polyhedron. The approximation error is verified by comparison with the exact volume of the polyhedron provided by the Gauss divergence theorem. Voxelization of the polyhedron interior is achieved by the aid of an indicator function, which is very similar to the signed distance to the boundary of the polyhedron. The proposed numerical method can be used in 3D quantification of glenoid bone loss.

Keywords: Polyhedron · Volume computation · Glenoid bone loss.

1 Introduction

Studies show that about 90% of shoulder joints with recurrent anterior shoulder dislocation have an abnormal glenoid shape [13]. The preoperative assessment of anterior glenoid bone loss is a critical step in surgical planning for patients with recurrent anterior glenohumeral instability. The currently accepted gold standard for glenoid structural assessment among most orthopaedic surgeons is the use of 3-dimensional reconstructed computed tomography images with the humeral head digitally subtracted, yielding an en face sagittal oblique view of the glenoid. Several methods have been reported to quantify the amount of glenoid bone loss [4]. One of the most commonly used concepts described in the literature uses the diameter of the "best-fit circle" circumscribed around the inferior glenoid. To quantify the amount of glenoid bone loss, reported as a percentage of either total surface area or diameter, the following measures are used for the diameter-based method and surface area method, respectively: Percent bone loss = (Defect width/Diameter of inferior glenoid circle) $\times$ 100% and Percent bone loss = (Defect surface area/Surface area of inferior glenoid circle) $\times$ 100%. Comparison of the diameter-based method and surface area method is carried out in Table 1 in [4].

* Supported by the Research Executive Agency of the European Commission, grant 778035 - PDE-GIR - H2020-MSCA-RISE-2017.

To measure glenoid bone loss, surgeons typically use radiographs and 2D CT scans and apply the surface area method, where certain part of the glenoid bone is positioned within the best-fit circle and the missing area in the circle represents size of the bone defect; see Fig. 1a.

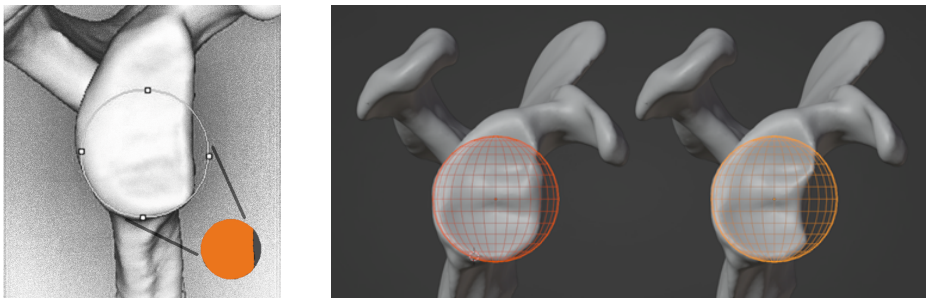

(a) (b)

Fig. 1. (a) Best-fit circle method for evaluation of glenoid bone defect. (b) 3D volume measurement of a glenoid bone

Magnetic resonance imaging (MRI) has been the gold standard for visualizing soft tissue lesions, but it has also proven to be an accurate modality for measuring glenoid bone loss in recent clinical studies [3, 12, 15]. With the development of three-dimensional bone reconstruction technologies, more accurate measurements are being explored, for example, using the best-fit spherical volume instead of the circle area method. By placing the evaluated bone area inside a sphere and measuring the difference between the reconstructed bone and the interior of the sphere, the bone defect is evaluated in terms of 3D volume instead of 2D area; see Fig. 1b.

In the present paper, we describe a numerical method for measuring the volume portion of a bone inside a given 3D sphere. Our contribution is a careful selection of fast and robust algorithms for this method and a posteriori accuracy test for the computed result. The design of the numerical method was inspired by [6] and can be considered as a simpler alternative to the algorithm in [1] equipped with the accuracy test.

2 Statement of the Problem

We are given a three-dimensional solid object B, such as the glenoid bone, embedded into a three-dimensional parallelepiped Ω. The boundary ∂B of B is assumed to be a two-dimensional triangulated surface without boundary, i.e. it consists of plane triangles and is watertight. The triangulation of ∂B is given in the STL format by means of three matrices P, T and F, which denote respectively the set of vertices, the triangulation connectivity list and the set of outward unit face normals. The i-th row of the real $N \times 3$ matrix P contains

the coordinates of vertex i. The k-th row of the integer $K \times 3$ matrix T contains the vertex numbers for the k-th triangle. The k-th row of the real $K \times 3$ matrix F contains the outward unit normal n_k to the k-th triangle. Orientation of the k-th triangle given by the row k of T is consistent with the direction of the normal vector n_k. Recall that a solid object inside a triangulated surface is usually referred to as a polyhedron.

Intersection of a polyhedron with a ball. Consider a three-dimensional open ball $C = \{x \in R^3 \colon \|x - a\|_2 < r\}$, where $a \in R^3$ is a center, $r > 0$ is a radius and $\|v\|_2 = \sqrt{v_1^2 + v_2^2 + v_2^2}$ is the Euclidean vector norm.

Our main problem is how to compute the volume of the intersection $B \cap C$. It is worth emphasizing here that we do not need to evaluate this volume exactly or with high accuracy. For example, a relative error not exceeding one percent may be quite satisfactory.

3 Volume of a Polyhedron via the Gauss Formula

The Gauss-Ostrogradsky divergence theorem for a function $f(v) = (f_1, f_2, f_3)^T$ of $v = (x_1, x_2, x_3)^T$ reads

$$\int_B \left(\frac{\partial f_1}{\partial x_1} + \frac{\partial f_2}{\partial x_2} + \frac{\partial f_3}{\partial x_3} \right) dv = \int_{\partial B} (f_1 n_1 + f_2 n_2 + f_3 n_3)\, ds, \tag{1}$$

where $n = (n_1, n_2, n_3)^T$ is the outward unit normal to the surface ∂B and ds is the surface area element. If $f = (0, 0, x_3)$, then $\int_B dv = \int_{\partial B} x_3 n_3 ds$. Each triangle $T^{(k)}$ in ∂B is given by a sequence of vertex vectors $p_1^{(k)}, p_2^{(k)}, p_3^{(k)}$ ordered consistently with the outward unit normal $n^{(k)}$. Let us denote by $m_3^{(k)}$ the third component of the mean vector $(p_1^{(k)} + p_2^{(k)} + p_3^{(k)})/3$. It follows that $\int_{\partial B} x_3 n_3 ds = \sum_k m_3^{(k)} n_3^{(k)} \mathrm{area}(T^{(k)})$. The vector product $w^{(k)} = (w_1^{(k)}, w_2^{(k)}, w_3^{(k)})^T$ of the vectors $p_2^{(k)} - p_1^{(k)}$ and $p_3^{(k)} - p_2^{(k)}$ satisfies $w^{(k)} = \|w^{(k)}\|_2 n^{(k)}$ and $\|w^{(k)}\|_2 = 2\,\mathrm{area}(T^{(k)})$. Hence the volume of B equals

$$V = \int_B dv = \frac{1}{2} \sum_k m_3^{(k)} w_3^{(k)}. \tag{2}$$

More formulas derived by means of the divergence theorem are found in [10].

4 The Voxelization Approach

The ideal (exact) method could be to describe the boundary of the intersection $B \cap C$ exactly and apply a variant of the Gauss divergence formula similar to (2). However, theoretical derivation of this method seems to be too involved. Alternatively, one can try to use results from the advanced theory of boolean operations with polyhedra, see e.g. [16, 14, 5, 8].

Since we admit approximate evaluation of the volume of $B \cap C$, we follow a much simpler approach based on the so called voxelization of the solid object. Namely, having defined a uniform 3-D mesh $\mathcal{M}$ in the parallelepiped Ω containing the object B, we find the set $\mathcal{M}_i$ of all interior points of $\mathcal{M}$, i.e. the mesh points belonging to B. Let us denote the number of interior points by $|\mathcal{M}_i|$. Assume that a single voxel in $\mathcal{M}$ is a cube with the side length h so that its volume equals h^3. Then the product $h^3|\mathcal{M}_i|$ approximates the volume of object B. The approximation error converges to zero as $\text{area}(\partial B)O(h)$ at most, where $\text{area}(\partial B)$ is the surface area of ∂B. Note that the voxelization approach is also used for more complicated problems such as boolean operations with polyhedra, see e.g. [11].

The volume of $B \cap C$ is approximated by $h^3|\mathcal{M}_i \cap C|$, where $|\mathcal{M}_i \cap C|$ is the number of interior mesh points inside the ball C.

The main problem in our voxelization approach is the 3-D point location problem that is the determination whether $x \in B$ or not for any point $x \in \Omega$. There exist efficient combinatorial solutions such as the method developed in [7]. We choose the more widespread tools based on the distance maps and the closest neighbor maps combined with the outward surface normals. Namely, we take advantage of the indicator function from Section 5. This indicator function has been used, for instance, in [1, 6].

5 Description of Our Numerical Method

We use the level set method, in which the surface ∂B is represented by the 0-level set of a function $u(x)$, i.e. $\partial B = \{x \in \Omega \colon u(x) = 0\}$. Moreover, we want to construct $u(x)$ such that $u(x) < 0$ inside B and $u(x) > 0$ outside B. Let us call a function $u(x)$ satisfying these properties an indicator function.

The numerical method consists of the following steps:

- Read the STL data for the surface ∂B.
- Sample (discretize) the surface ∂B into a 3D point cloud $\mathcal{P}$ with outward normals.
- Determine a 3D parallelepiped Ω enclosing the point cloud $\mathcal{P}$ and choose a uniform grid $\mathcal{M}$ in Ω of voxel size h.
- Downsample the point cloud $\mathcal{P}$ onto the grid points of $\mathcal{M}$.
- Compute the closest point map for all grid points of $\mathcal{M}$ with the closest points in the downsampled point cloud.
- Compute the distance map to the downsampled point cloud for all grid points of $\mathcal{M}$.
- Compute the indicator function $u(x)$.
- Remove (possible) impulse noise by the median filter or by the TVG-L1 filter.
- Determine the interior grid points in B by zero thresholding $u(x)$.
- Compute the volume of B as the number of interior points times h^3 and compare it with the volume defined by the divergence theorem.

– Determine the number of interior points lying in C and calculate the volume of the intersection $B \cap C$.

Let us look at these steps in more detail below.

5.1 Randomized Sampling of the Surface

In contrast to [1], where the Euclidean distance map is computed with respect to the triangulated surface, we sample the triangulated surface into a point cloud. Such decision is mainly due to the further use of standard efficient algorithms for computation of the distance map.

We simply choose several points randomly on each triangle $T^{(k)}$ of the triangulation and use the same normal vector $n^{(k)}$ for all of them. The number of chosen points depends on the precomputed area of $T^{(k)}$ in order to get sufficiently dense sampling of the surface.

5.2 Downsampling the Point Cloud

The continuous solid object is discretized on a uniform regular 3D grid $\mathcal{M}$. We specify a grid number for the space direction that has the largest range and the other two will be determined by their related range. The voxels are cubes with the side length h.

To speed up the computation, a simple downsampling preprocessing based on the interpolation to the closest neighbor on the grid $\mathcal{M}$ is applied. By such a preprocessing, the quality of the resulting point cloud does not change when h is sufficiently small.

5.3 Distance Function and Closest Point Map

The distance function, or the distance map, of a point $x \in \Omega$ to a point set $\mathcal{P} = \{p_i\}_{i=1}^{N}$ is defined as

$$d(x) = \min_i \|x - p_i\|. \tag{3}$$

We use the Euclidean norm in (3). Note that $d(x) \geq 0$ and $d(x)$ is exactly 0 at the point cloud. The function `bwdist` in MATLAB implements the algorithm from [9] for computation of $d(x)$.

A very useful byproduct of the distance function is the closest point map. At a point $x \in \Omega$, we denote by $\mathrm{cp}(x)$ the point $p_i \in \mathcal{P}$ that is closest to x,

$$\mathrm{cp}(x) = \arg\min_i \|x - p_i\|. \tag{4}$$

5.4 Indicator Function

Assume that all points in the cloud $\mathcal{P}$ have a unit outward normal. For any $x \in \Omega$, we define the indicator function

$$f(x) = (x - \mathrm{cp}(x)) \cdot n(\mathrm{cp}(x)), \tag{5}$$

which equals the dot product of the vector $x - \mathrm{cp}(x)$ with the unit outward normal $n(\mathrm{cp}(x))$ at $\mathrm{cp}(x)$. The indicator function $f(x)$ is negative when x is inside B and positive when x is outside B. The function (5) is called the inner product field in [6]. The function $\mathrm{sign}(f(x))d(x)$ is computed exactly for polyhedra in [1] and called the signed distance function there.

5.5 Denoising

The indicator function $f(x)$ in (5) is not stably defined when the vectors $x - \mathrm{cp}(x)$ and $n(\mathrm{cp}(x))$ are orthogonal or almost orthogonal. Therefore, $f(x)$ can be subject to impulse noise in such locations x. The noise is removed by the median filter.

More expensive denoising filter TVG-L1 is proposed in [2]. It produces a smoother 0-level set of $f(x)$ than the median filter. We remark that the median filter provides a quite satisfactory result because our goal is computing the volume of B, not the boundary ∂B. Moreover, the use of $f(x)$ without denoising is often satisfactory. A test of accuracy is given in Section 5.6.

The TVG-L1 filter applied to $f(x)$ is a solution $u(x)$ of the variational model

$$\min_u \int_\Omega g(x)|\nabla u(x)| + \lambda|u - f|dx, \tag{6}$$

where $g(x) > 0$ is a weight function and λ is a suitable smoothing parameter. Solving (6) directly is not easy, therefore, it is often approximated by the easier variational model

$$\min_{u,v} \int_\Omega \left(g(x)|\nabla u| + \lambda|v| + \frac{1}{2\theta}|u + v - f|^2 \right) dx, \tag{7}$$

which converges to (6) for sufficiently small $\theta > 0$. We use $g(x) = d(x)$. A numerical algorithm for solving (7) is found in [2, 6]. In our implementation, the distance function and indicator function are scaled to be ranged over the interval $[0, 1]$ and then we set $\lambda = 0.01$ and $\theta = 0.05$ as in [6].

5.6 Test of Accuracy

The set of interior grid points of $\mathcal{M}$ in B is $\mathcal{M}_i = \{x \in \mathcal{M} \colon f(x) < 0\}$, or $\mathcal{M}_i = \{x \in \mathcal{M} \colon u(x) < 0\}$ after denoising. An approximate volume of B equals $h^3|\mathcal{M}_i|$, where $|\mathcal{M}_i|$ is the number of points in $\mathcal{M}_i$. We compare $h^3|\mathcal{M}_i|$ with the exact volume computed by (2). If the relative error is not small enough, the computation of $f(x)$ and $u(x)$ is repeated with a smaller voxel size h.

Finally, we can calculate the number of points from $\mathcal{M}_i$ that belong to the ball B and multiply it by h^3 in order to get the volume of the intersection $B \cap C$.

6 Numerical Illustration

Two examples have been computed in MATLAB to examine the proposed numerical method: one for a normal glenoid bone and another for a defective one. The examples are quite similar so we present only results for a defective glenoid bone. The exact volume of the whole bone evaluated from the STL data by the Gauss formula equals 1.99161. The exact area of the bone surface equals 25.6750. The computed approximate volume of the bone amounts to 1.99281 before denoising, to 1.98723 after denoising with the median filter and to 1.99284 after denoising with the TVG-L1 filter. The uniform grid $\mathcal{M}$ is of size $161 \times 225 \times 283$ and has the voxel size $h = 0.0169$. The number of cloud points on the boundary after downsampling is 124190. Arithmetical complexity of the proposed numerical method is $O(|STL|) + O(|\mathcal{M}|)$, where $|STL|$ is the length of all STL data and $|\mathcal{M}|$ is the number of voxels in Ω.

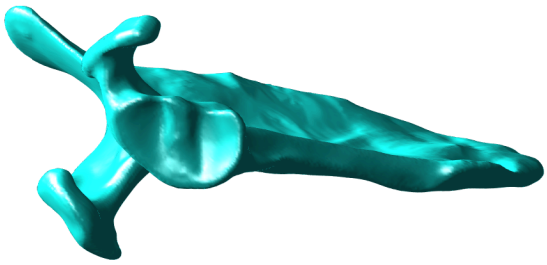

Fig. 2. 0-level of the denoised indicator function computed by the MATLAB function `isosurface`

7 Conclusion

We have developed a simple method for computing the volume of the intersection of a three-dimensional ball with a polyhedron given by a triangulated closed surface and outward unit normals. The method is based on voxelization of the interior of the polyhedron and uses the closest point map to a sufficiently fine sampling of the triangulated surface. Arithmetic complexity of the method is linear with respect to the number of voxels in a parallelepiped containing the polyhedron. The computed volume is approximate but its accuracy is guaranteed by a posteriori estimate calculated with the help of the Gauss-Ostrogradsky divergence theorem.

References

1. Bærentzen, J.A., Aanæs, H.: Signed distance computation using the angle weighted pseudonormal. IEEE Transactions on Visualization and Computer Graphics **11**(3), 243–253 (2005). https://doi.org/10.1109/TVCG.2005.49

2. Bresson, X., Esedoglu, S., Vanderheynst, P., Thiran, J.P., Osher, S.: Fast global minimization of the active contour/snake model. J. Math. Imaging Vis. **28**, 151–167 (2007). https://doi.org/10.1007/s10851-007-0002-0
3. Gyftopoulos, S., Beltran, L.S., Yemin, A., et al.: Use of 3D MR reconstructions in the evaluation of glenoid bone loss: a clinical study. Skeletal Radiology **43**, 213–218 (2014). https://doi.org/10.1007/s00256-013-1774-5
4. Hamamoto, J.T., Leroux, T., Chahla, J., et al.: Assessment and evaluation of glenoid bone loss. Arthroscopy Techniques **5**(4), e947–e951 (2016). https://doi.org/10.1016/j.eats.2016.04.027
5. Jiang, X., Peng, Q., Cheng, X., et al.: Efficient Booleans algorithms for triangulated meshes of geometric modeling. Computer-Aided Design & Applications **13**(4), 419–430 (2016). https://doi.org/10.1080/16864360.2015.1131530
6. Liang, J., Park, F., Zhao, H.: Robust and efficient implicit surface reconstruction for point clouds based on convexified image segmentation. J. Sci. Comput. **54**, 577–602 (2013). https://doi.org/10.1007/s10915-012-9674-8
7. Magalhães, S.V., Andrade, M.V., Franklin, W.R., Li, W.: PinMesh—fast and exact 3D point location queries using a uniform grid. Computers & Graphics **58**, 1–11 (2016). https://doi.org/10.1016/j.cag.2016.05.017
8. Magalhães, S.V., Franklin, W.R., Andrade, M.V.: An efficient and exact parallel algorithm for intersecting large 3-D triangular meshes using arithmetic filters. Computer-Aided Design **120**(102801), 1–11 (2020). https://doi.org/10.1016/j.cad.2019.102801
9. Maurer, C., Qi, R., Raghavan, V.: A linear time algorithm for computing exact euclidean distance transforms of binary images in arbitrary dimensions. IEEE Transactions on Pattern Analysis and Machine Intelligence **25**(2), 265–270 (2003). https://doi.org/10.1109/TPAMI.2003.1177156
10. Mirtich, B.: Fast and accurate computation of polyhedral mass properties. Journal of Graphics Tools **1**(2), 31–50 (1996). https://doi.org/10.1080/10867651.1996.10487458
11. Pavić, D., Campen, M., Kobbelt, L.: Hybrid Booleans. Computer Graphics Forum **29**(1), 75–87 (2010). https://doi.org/10.1111/j.1467-8659.2009.01545.x
12. e Souza, P.M., Brandão, B.L., Brown, E., et al.: Recurrent anterior glenohumeral instability: the quantification of glenoid bone loss using magnetic resonance imaging. Skeletal Radiol. **43**, 1085–1092 (2014). https://doi.org/10.1007/s00256-014-1894-6
13. Sugaya, H., Moriishi, J., Dohi, M., Kon, Y., Tsuchiya, A.: Glenoid rim morphology in recurrent anterior glenohumeral instability. J. Bone & Joint Surg. **85**(5), 878–884 (2003). https://doi.org/10.2106/00004623-200305000-00016
14. Xiao, Z., Chen, J., Zheng, Y., Zheng, J., Wang, D.: Booleans of triangulated solids by aboundary conforming tetrahedral mesh generation approach. Computers & Graphics **59**, 13–27 (2016). https://doi.org/10.1016/j.cag.2016.04.004
15. Yanke, A.B., Shin, J.J., Pearson, I., et al.: Three-dimensional magnetic resonance imaging quantification of glenoid bone loss is equivalent to 3-dimensional computed tomography quantification: Cadaveric study. Arthroscopy: The Journal of Arthroscopic & Related Surgery **33**(4), 709–715 (2017). https://doi.org/10.1016/j.arthro.2016.08.025
16. Zhou, Q., Grinspun, E., Zorin, D., Jacobson, A.: Mesh arrangements for solid geometry. ACM Transactions on Graphics **35**(4), Article No. 39, 1–15 (2016). https://doi.org/10.1145/2897824.2925901